Wheat genome architecture influences interactions with phytobeneficial microbial functional groups in the rhizosphere

Cécile Gruet, Danis Abrouk, Andreas Börner, Daniel Muller, Yvan Moënne-Loccoz

Wheat genome architecture influences interactions with phytobeneficial microbial functional groups in the rhizosphere

Cécile Gruet[1], Danis Abrouk[1], Andreas Börner[2], Daniel Muller[1], Yvan Moënne-Loccoz[1]

[1]Univ Lyon, Université Claude Bernard Lyon 1, CNRS, INRAE, VetAgro Sup, UMR5557 Ecologie Microbienne, 43 bd du 11 Novembre 1918, 69622 Villeurbanne, France

[2]Genebank Department, Leibniz Institute of Plant Genetics and Crop Plant Research (IPK), Corrensstr. 3, 06466 Seeland OT Gatersleben, Germany

Correspondence

Yvan Moënne-Loccoz, Université Claude Bernard Lyon 1, UMR5557 Ecologie Microbienne, 43 bd du 11 Novembre 1918, 69622 Villeurbanne, France

Email: yvan.moenne-loccoz@univ-lyon1.fr

ORCID

Cécile Gruet 0000-0001-8667-0838

Danis Abrouk 0000-0002-7162-5388

Andreas Börner 0000-0003-3301-9026

Daniel Muller 0000-0002-6619-4691

Yvan Moënne-Loccoz 0000-0002-9817-1953

Running title: Wheat genome and microbial functional groups

Abstract

Wheat has undergone a complex evolutionary history, which led to allopolyploidization and the hexaploid bread wheat *Triticum aestivum*. However, the significance of wheat genomic architecture for beneficial plant-microbe interactions is poorly understood, especially from a functional standpoint. In this study, we tested the hypothesis that wheat genomic architecture was an overriding factor determining root recruitment of microorganisms with particular plant-beneficial traits. We chose five wheat species representing genomic profiles AA (*Triticum urartu*), BB {SS} (*Aegilops speltoides*), DD (*Aegilops tauschii*), AABB (*Triticum dicoccon*) and AABBDD (*Triticum aestivum*) and assessed by qPCR their ability to interact with free-nitrogen fixers, 1-aminocyclopropane-1-carboxylate deaminase producers, 2,4-diacetylphloroglucinol producers and auxin producers via the phenylpyruvate decarboxylase pathway, in combination with Illumina MiSeq metabarcoding analysis of N fixers (and of the total bacterial community). We found that the abundance of the microbial functional groups could fluctuate according to wheat genomic profile, as did the total bacterial abundance. N fixer diversity and total bacterial diversity were also influenced significantly by wheat genomic profile. Often, rather similar results were obtained for genomes DD (*Ae. tauschii*) and AABBDD (*T. aestivum*), pointing for the first time that the D genome could be particularly important for wheat-bacteria interactions.

KEYWORDS

ACC deaminase producers, auxin producers, diazotrophs, holobiont, microbial functional groups, plant-bacteria interactions.

1. INTRODUCTION

Along with rice and maize, durum wheat and especially bread wheat are major crops for human nutrition. The importance of wheat stems from its capacity to be cultivated in various parts of the world, across a wide range of soil and climatic conditions (Willcox, 2005; Haas *et al.*, 2019). Accordingly, wheat is exposed to contrasted microbial communities, as the soil microbiome displays strong biogeographic patterns (Nemergut *et al.*, 2011; Bru *et al.*, 2011; Karimi *et al.*, 2018; Bay *et al.*, 2020).

Wheat has undergone a complex evolutionary history, which involved several events of genomic hybridization and subsequent domestication (Feldman & Kislev, 2007; Asouti & Fuller, 2012; Marcussen *et al.*, 2014; Haberer *et al.*, 2016; Baidouri *et al.*, 2017; Pont *et al.*, 2019; Glémin *et al.*, 2019). These multiple hybridizations took place between different *Triticum* and *Aegilops* species (Figure 1), and led to allopolyploidization (*i.e.* the addition of parental genomes) (Soltis & Soltis, 2000). Thus, *Triticum urartu* (AA genome) and an unknown BB-genome *Aegilops* having *Aegilops speltoides* (SS genome) as ancestor hybridized and yielded wild emmer *Triticum dicoccoides* (AABB genome), from which *Triticum dicoccon* and then durum wheat *Triticum durum* (both with AABB genome) derived (Özkan *et al.*, 2011). In addition, *T. dicoccon* and *Aegilops tauschii* (DD genome) hybridized to form an unknown AABBDD-genome wild wheat, which gave bread wheat *Triticum aestivum* (AABBDD genome) after domestication (Salamini *et al.*, 2002). Genomic hybridization and polyploidization are extensively documented in plants, albeit not to such extent in the other *Poaceae* (Paterson *et al.*, 2004; Wei *et al.*, 2007; Messing, 2009).

Genomic hybridization and polyploidization may have strong impacts on (i) plant adaptation, e.g. through the possibility to evolve new functions (Soltis & Soltis, 2000; Soltis *et al.*, 2015), and (ii) plant physiology via, in particular, epigenetic effects (Jackson, 2017).

Since each gene is present in several copies, it can possibly lead to sub-functionalization (all copies evolve to become complementary), neo-functionalization (one copy gains a new function) or non-functionalization (one copy is not functional anymore) (Soltis *et al.*, 2015). Polyploidization is thought to confer ecological benefits (Soltis & Soltis, 2000; Soltis *et al.*, 2015). Polyploids display a patchwork of parental and new characteristics, including for traits influencing plant-microbe interactions such as root exudation, root uptake patterns, etc. (Saia *et al.*, 2019; Iannucci *et al.*, 2021; Gruet *et al.*, 2022a).

In soil, plant roots interact with a myriad of microorganisms (Moënne-Loccoz *et al.*, 2015), many of them being beneficial or deleterious to the plant (Vacheron *et al.*, 2013; Parnell *et al.*, 2016; Nowell *et al.*, 2016). Therefore, microbial interactions are important factors modulating wheat performance (Narula *et al.*, 2000; Glick, 2014; Majeed *et al.*, 2015; Pérez-de-Luque *et al.*, 2017; Bernardo *et al.*, 2019; Dellagi *et al.*, 2020), and it is likely that these interactions could have influenced the selection of wheat genotypes at the different stages of its evolutionary history (Gruet *et al.*, 2022a). However, data available on this issue is scarce. Wheat species of different genomic architectures have been compared, with a focus on bacterial taxonomic diversity (Ito *et al.*, 2020), which limited the possibility to consider plant-beneficial traits harbored by rhizosphere bacteria. Functional aspects of the bacterial microbiome, also, might depend on the genomic traits of wheat, and this hypothesis was investigated here.

The objective of this study was to assess whether wheat genotypes of contrasting genomic architectures differ in their ability to interact with functional microbial groups important for plant growth. To this end, wheat species of genomic profiles AA (*T. urartu*, wild), SS (*A. speltoides*, wild; SS is the closest genome to BB that is currently available), DD (*Ae. tauschii*, wild), AABB (*T. dicoccon*, domesticated) and AABBDD (*T. aestivum*, domesticated) (Figure 1) were grown in a same soil. Their ability to recruit key plant-

beneficial functional groups (*i.e.* all microorganisms performing a same function) was assessed based on qPCR and/or MiSeq sequencing. The focus was put on four prominent groups, *i.e.* (i) free nitrogen fixers (by targeting the nitrogenase gene *nifH* involved in N_2 fixation) (Poly *et al.*, 2001), (ii) 1-aminocyclopropane-1-carboxylate (ACC) deaminase producers (*acdS*; cleavage of the ethylene precursor ACC) (Glick, 2005, 2014), (iii) producers of the auxinic-type root-branching signal 2,4-diacetylphloroglucinol (DAPG) (polyketide synthase gene *phlD*) (Brazelton *et al.*, 2008), and (iv) *ppdC*$^+$ 3-indole acetic acid (IAA) producers (phenylpyruvate decarboxylase gene *ppdC*) (Spaepen *et al.*, 2007b; Zhao, 2014; Gruet *et al.*, 2022b), based on their importance for plant performance and the availability of molecular tools. In addition, the total bacterial community was also monitored, using the 16S rRNA gene *rrs*, to assess whether trends at the level of individual functional groups were also relevant at the scale of the entire community.

2. MATERIALS AND METHODS

2.1. Plant material

For each of the five species *T. urartu*, *T. dicoccon*, *T. aestivum*, *Ae. speltoides* and *Ae. tauschii*, four contrasted genotypes (Table S1; *i.e.* : TU8, TU9, TU2, TU7 for *T. urartu*, AS7, AS3, AS1, AS8 for *Ae. speltoides*, TD9, TD0, TD3, TD1 for *T. dicoccon*, AT5, AT0, AT9, AT1 for *Ae. tauschii*, and AE4, AE2, AE3, AE6 for *T. aestivum*) were selected from the wheat collection of the Leibniz Institute of Plant Genetics and Crop Plant Research (Gatersleben, Germany), based on passport data available. All seeds used in the experiment were produced in the same fields at Gatersleben.

2.2. Greenhouse experiment and plant sampling

Wheat lines were cultivated in soil originating from the loamy surface horizon (clay 16%, silt 44%, sand 40%; 2.1% organic matter, pH 7, cation exchange capacity 8.2 $cmol.kg^{-1}$) of a luvisol located at La Côte Saint-André near Lyon (France) and kept for decades as a permanent meadow. The soil was sieved at 6 mm and evenly mixed before preparing pots (2.5 kg soil per 3-dm^3 pot).

Before sowing, wheat seeds were surface-disinfected by soaking 30 min in 1.2% sodium hypochlorite solution, rinsed five times with sterile demineralized water, and soaked in sterile water for one hour. Six replicates (i.e. six pots) were used for each wheat line, with four seeds per pot (thinned to two seedlings on day 10). Six non-planted pots were also included as controls. The pots were placed following a randomized block design (6 blocks) in a greenhouse with 16 h of light (25°C) and 8 h of darkness (18°C). Blocks and pots within the blocks were regularly moved around to minimise greenhouse heterogeneity effects. Every two days, water was poured to the surface of the soil to adjust water content to soil retention capacity (21% w/w).

Ae. tauschii, *T. dicoccon* (except genotype TD0) and *T. aestivum* were sampled at 14 and 40 days of growth, whereas *T. dicoccon* TD0, *T. urartu* and *Ae. speltoides* were only sampled at 40 days because their growth at 14 days was still limited. In addition, *T. urartu* genotype TU9 underwent wilting and could not be included in the study. Whole root systems were recovered to consider possible growth fluctuations between genotypes, as recommended (Simmons *et al.*, 2018), and they were shaken to remove loosely-adhering soil. Roots and tightly-adhering soil were frozen in liquid nitrogen and lyophilized for 48 h. After lyophilisation, root-adhering soil was separated from roots (by removing every root piece with tweezers) and placed at -80°C until DNA extraction. Shoots were also sampled and dried at 50°C for 4 days, and shoot dry weight was measured. Soil from non-planted pots was also frozen in liquid nitrogen, lyophilized and kept at -80°C.

151 **2.3. DNA extraction from soil**

152 Nucleic acid extraction was done as described by Bouffaud *et al.* (2014) from 0.5 g of
153 rhizosphere or bulk soil. Briefly, frozen soil was homogenized using a vortex and 0.5 g (for
154 standardization) of bulk or rhizosphere soil were taken from the total amount of soil. Then,
155 0.5 mL of zirconium beads (VWR, Fontenay-sous-Bois, France), 0.5 mL of extraction buffer
156 (5% hexadecyltrimethylammonium bromide and 1 mM 1,4-dithio-DL-threitol in a 0.12 M
157 phosphate buffer at pH 8.0) and 0.5 mL of phenol-chloroform-isoamyl alcohol (24:24:1 v/v/v)
158 were added to soil, and they were mixed in a bead beater (TissueLyser II Retsch;
159 Courtaboeuf, France) for 90 s at 30 m s^{-1} and centrifuged for 10 min at 16,000 *g*. Supernatants
160 were extracted a second time in phenol-chloroform-isoamyl alcohol and once in chloroform-
161 isoamyl alcohol (24:1 v/v). Nucleic acids were precipitated overnight with a 3 M potassium
162 acetate solution at pH 4.8 and absolute ethanol at -20°C. After centrifugation for 30 min at
163 16,000 *g*, pellets were washed in 70% cold ethanol and dissolved in 60 µL RNase-free water.
164 Extracted nucleic acids were quantified using a Nanophotometer NP80 (Implen GmbH;
165 Munich, Germany) and results were expressed in ng μL^{-1}. Very similar DNA yields were
166 obtained from every sample.
167
168 **2.4. qPCR analyses of *rrs* and functional genes *nifH, acdS, ppdC* and *phlD***
169 qPCR is a method of reference for quantify root-associated microorganisms *(*Hou *et al.*, 2021*;*
170 Wippel *et al.*, 2021; Liu *et al.*, 2022; Cadot *et al.*, 2021). The size of the total bacterial
171 community and of four functional groups (free nitrogen fixers, ACC deaminase producers,
172 *ppdC*$^{+}$ IAA producers and DAPG producers) was estimated by quantitative PCR, at 14 days
173 of growth for *T. dicoccon*, *Ae. tauschii* and *T. aestivum*, and 40 days for bulk soil and for all
174 five wheat species. qPCR reactions for the corresponding genes (*rrs*, *nifH, acdS, ppdC* and
175 *phlD*, respectively) were performed in 20 µL containing 10 µL of LightCycler-DNA Master

SYBR Green I master mix (Roche Applied Science, Penzberg, Germany), 2 µL of sample DNA (10 ng DNA), and primers 519F/907R for *rrs* (0.6 µL, to reach a final concentration of 0.6 µM), 3F*ppdC*/3R*ppdC* for *ppdC* (0.6 µL, final concentration 0.6 µM), *pol*F/*pol*R for *nifH* (2 µL, final concentration 0.5 µM), *acc*F5/*acc*R8 for *acdS* (1 µL, final concentration 1 µM) or B2BR3/B2BF for *phlD* (1 µL, final concentration 1 µM). PCR-grade water was added to reach 20 µL. All primers pairs and references are shown in Table S2. The *nifH* primers *pol*F/*pol*R are recommended to quantify diazotrophs (Gaby and Buckley, 2017). Primers amplify *nifH*, *ppdC* and *phlD* from prokaryotes, whereas for *acdS* a minority of fungal sequences may also be recovered. Testing of *rrs* primers 519F/907R by Illumina MiSeq sequencing (see 2.5 below for procedures), using one replicate of *T. aestivum* line AE6, *T. dicoccon* line TD3 and *T. urartu* line TU2 at 40 days identified only 1.77% (*T. aestivum*) to 5.74% (*T. urartu)* of chloroplast or mitochondria sequences (mean 4.64%), leading to a negligible overestimate of 0.02 $\log_{10}$ units on average (and 0.03 $\log_{10}$ units for *T. urartu*) for qPCR values that ranged from 6.3 to 8.7 $\log_{10}$ bacteria per g of rhizosphere soil (see 3.1 below).

For each targeted gene, the cycling program included an initial activation step of 10 min at 95°C, and the specificity of the amplification was verified by melting curve analysis, assessed by increasing the temperature from 65°C to 95°C, at a rate of 0.1°C s^{-1}. For *rrs*, 40 cycles of amplification were done (10 s at 95°C, 50 s at 63°C, 30 s at 72°C) and the standard curve was generated using a plasmid containing one copy of *rrs*, after dilution from 10^6 to 10 copies. For *nifH*, 50 cycles of amplification were done (10 s at 95°C, 15 s at 64°C, 15 s at 72°C) and the standard curve was generated using genomic DNA of *Azospirillum* (ex *brasilense*) *baldaniorum* Sp245, after dilution from 5×10^{-9} to 5×10^{-14} g DNA μL^{-1} (corresponding to 1.5×10^6 to 15 copies, respectively). For *acdS*, 50 cycles of amplification were done (15 s at 95°C, 15 s at 67°C, 10 s at 72°C) and the standard curve was generated

using genomic DNA of *Burkholderia cenocepacia* J2315, after dilution from 5×10^{-9} to 5×10^{-14} g DNA μL^{-1} (corresponding to 1×10^{6} to 10 copies, respectively). For *ppdC*, 50 cycles of amplification were done (15 s at 95°C, 15 s at 63°C, 10 s at 72°C) and the standard curve was generated using genomic DNA of *Ae. baldaniorum* Sp245, after dilution from 5×10^{-9} to 5×10^{-14} g DNA μL^{-1} (corresponding to 1.5×10^{6} to 15 copies, respectively). Lastly, for *phlD*, 50 cycles of amplification were done (30 s at 95°C, 7 s at 67°C, 15 s at 72°C) and the standard curve was generated using genomic DNA of *Pseudomonas* (ex *fluorescens*, ex *kilonensis*) *ogarae* F113, after dilution from 3×10^{-9} to 3×10^{-14} g DNA μL^{-1} (corresponding to 9×10^{5} to 9 copies, respectively).

In order to verify possible bias linked to the presence of qPCR inhibitors, two samples for each targeted gene were diluted at 1/50, 1/100, 1/150, and 1/200. A curve was drawn for each sample to determine the dilution range in which the efficiency of amplification was between 80 and 100% (cycle threshold according to amplicon concentration).

Results expressed in g μL^{-1} were converted into numbers of copies using the formula [DNA (g) × Avogadro's number (molecules mol^{-1})]/[number of DNA bp in amplified fragments × 660 (g mol^{-1})], based on an average of 660 g mol^{-1} per base pair. They were normalized to the total DNA quantity extracted from 0.5 g of soil, and expressed into number of copies g^{-1} dry soil as previously done (Bouffaud *et al.* 2016, 2018; Ke *et al.*, 2019; Simonin *et al*., 2015, 2016, 2018; Renoud *et al.*, 2020). The size of the bacterial rhizosphere community was calculated taking into account that a given individual bacterium may contain several copies of *rrs*, ranging usually from 2 to 6 copies (Klappenbach *et al.*, 2001; Větrovský & Baldrian, 2013). An intermediate value of 4 copies was chosen to estimate community size, by dividing qPCR data by 4. To estimate the relative abundance of the four functional groups, the corresponding qPCR data were divided by the number of *rrs* copies for the same sample. All results were $\log_{10}$-transformed for subsequent analysis.

2.5. *rrs* and *nifH* sequencing from bulk soil and rhizosphere DNA

The diversity of the total bacterial community and of the free nitrogen fixers in rhizosphere and bulk soil sampled at 40 days was assessed by Illumina MiSeq sequencing (2 × 300 bp) of *rrs* and *nifH* amplicons, respectively. DNA extracts were sent to MolecularResearch (MR) DNA laboratory (www.mrdnalab.com; Shallowater, Texas, USA) for sequencing. Primers 515F/806R (targeting the V4 region of *rrs* gene) (Caporaso *et al.*, 2011) and Zehr-nifHf/Zehr-nifHr (for *nifH*) (Zehr & McReynolds, 1989) were used for the sequencing library, the forward primer carrying a barcode. These *nifH* primers were not used for qPCR (see above) as they are too degenerated (Gaby and Buckley, 2017). For each gene, a 30-cycles PCR was achieved using the HotStarTaq Plus Master mix (Qiagen; Valencia, California, USA) with 3 min at 94°C, followed by 30 cycles of 30 s at 94°C, 40 s at 53°C and 1 min at 72°C, with a final elongation step of 5 min at 72°C. Samples were pooled together in the same proportions and purified using calibrated Ampure XP beads (Beckman Coulter; Brea, California, USA). The DNA libraries were obtained with Illumina TruSeq DNA library protocol. Sequencing was carried out on a MiSeq following manufacturer's instructions.

Sequencing data were treated with UPARSE pipeline (Edgar, 2013). Sequences were depleted of barcodes, and sequences < 150 bp or with ambiguous base calls were removed. The remaining sequences were denoised, operational taxonomic units (OTUs) were generated (using UCLUST in standard default; Edgar, 2010) and chimeras were removed using UCHIME (Edgar *et al.*, 2011). Final OTUs were classified using BLASTn comparing OTUs to a database derived from RDPII and NCBI for both *rrs* and *nifH* sequencing (rdp.cme.msu.edu, ncbi.nlm.nihh.gov). For *rrs*, OTUs (*i.e.* genus to species level) were defined at 97% similarity, genera at 94.5%, families at 86.5%, orders at 82%, classes at 78.5% and phyla at 75% (Yarza *et al.*, 2014). For *nifH* also, the gene is highly conserved and carries taxonomic information (Achouak *et al.*, 1999; Gaby & Buckley, 2014; Kapili *et al.*, 2020),

and *nifH*-based OTUs were defined at 97% similarity, as done previously (Collavino *et al.*, 2014; Gaby *et al.*, 2017; Renoud *et al.*, 2020). 80% of *nifH*-based OTUs could be affiliated down to the species level, 13.5% to the genus level, and the rest could not. Results were generated as contingency tables used for subsequent analysis. Taxonomy bar plots were generated at the most informative taxonomic levels for *rrs* (*i.e.* phylum and genus) and *nifH* (*i.e.* class, family, genus and species) sequences, using the same similarity thresholds for both genes (Gaby *et al.*, 2017).

2.6. Statistical analysis

All analyses were done at $P < 0.05$, using R 4.0.3 software (https://www.r-project.org).

For qPCR results and sequence data, outliers were detected using the Grubbs' test (Grubbs, 1969; Burns *et al.*, 2005), based on number of gene copies and Bray-Curtis distance, respectively. For qPCR, at 14 days, this sorting removed one replicate of *Ae. tauschii* genotype AT0 for *rrs*, one replicate each of *T. dicoccon* TD1, *Ae. tauschii* AT0 and *T. aestivum* AE6 for *acdS*, and one replicate of *Ae. tauschii* AT0 and one replicate of *T. aestivum* AE2 for *ppdC*. At 40 days, one replicate each of *T. urartu* TU2 and TU7, *Ae. tauschii* AT0 and *T. aestivum* AE6 for *rrs*, one replicate each of *T. urartu* TU8, *Ae. speltoides* AS8, *T. dicoccon* TD9, TD3, TD1 and *Ae. tauschii* AT0 for *nifH*, one replicate each of *T. dicoccon* TD9, *Ae. tauschii* AT5, AT0 and *T. aestivum* AE5 for *acdS*, and one replicate each of *T. dicoccon* TD9, *Ae. tauschii* AT1 and *T. aestivum* AE2 for *ppdC*, were removed. For sequence data, two replicates of *Ae. speltoides* AS7 and of *T. dicoccon* TD9 were removed for *nifH* analysis.

For qPCR results, first an ANOVA approach with a nested fixed effects model, followed by Tukey's HSD tests, was used to compare wheat species, taking into account the variability between lines of a same species. Second, this approach was also carried out to

277 compare wheat lines belonging to a same species. Third, one-way ANOVA, followed by
278 Tukey's HSD tests, was performed to compare all wheat species with bulk soil, by
279 considering each wheat line as a replicate (*i.e*. using the means) for the corresponding species.
280 All data and residuals were checked, which showed normal distribution and homogeneity of
281 variance.

282 Sequence data were treated and filtered with the R package phyloseq, using a workflow
283 described previously (McMurdie & Holmes, 2013; Callahan *et al.*, 2015). For each wheat
284 species and line, rarefaction curves were generated to characterize sequencing depth. OTUs
285 retrieved (i) in less than 20% of the samples (i.e. less than 24 of the 122 samples) and (ii)
286 represented by no more than three sequences in the study were removed from the dataset. In
287 each sample, the sequence count for each OTU was divided by the total number of sequences
288 in that sample, and this normalization was done for the *nifH* and *rrs* datasets. α-Diversity was
289 investigated based on Shannon index, inverse Simpson index and observed richness. For these
290 indices, the same statistical approaches as for qPCR (i.e. nested ANOVA with two series of
291 Tukey's HSD tests, and one-way ANOVA with Tukey's HSD tests) were followed to
292 compare wheat species, wheat lines within species, as well as wheat and bulk soil.
293 Compositions of the total bacterial community and free nitrogen fixers were assessed for the
294 five wheat species, and bacterial taxa abundances were compared between species and bulk
295 soil by a one-way ANOVA followed by Tukey's HSD tests. The differences of structure and
296 taxonomic composition of the total rhizosphere bacterial community and of free nitrogen
297 fixers associated with the different wheat species and bulk soil were assessed using a
298 PERMANOVA/adonis ('vegan' package) on the same nested model as before (based on
299 variance comparison of Bray Curtis distances for the structure [Bray & Curtis, 1957], and on
300 differential taxa abundance for taxonomic composition), which was done with 10,000
301 permutations. Dissimilarities were visually represented using Non-metric MultiDimensional

Scaling (NMDS), where each point corresponds to one individual plant (replicate) of one wheat line or one bulk soil replicate, and statistical ellipses (i.e. confidence interval of 95% based on multivariate normal distribution) were calculated for bulk soil and each wheat species. A Between-Class Analysis (BCA) was also performed, following a factorial design where the inertia between lines of a same species is minimized and the inertia between lines of different species is maximized. After calculation of the contribution of OTUs to each axis of the factorial design, this allowed to identify OTUs most associated with each wheat species.

3. RESULTS

3.1. Abundance of the total bacterial community at 14 and 40 days

The different wheat genotypes grew well in the sieved soil chosen, and the level of variability for plant root biomass at 40 days was small (Table S5). At 14 days of growth of *Ae. tauschii*, *T. dicoccon* and *T. aestivum*, the size of the rhizobacterial community of individual plants ranged from 7.4 to 8.7 $\log_{10}$ bacteria per g of rhizosphere soil (Figure 2A). For each wheat species, the differences between genotypes were not significant. Bacterial community size in the rhizosphere of *T. dicoccon* was higher than in bulk soil, but the differences between wheat species were not significant.

At 40 days of growth, the size of the bacterial rhizosphere community varied from 6.3 to 8.1 $\log_{10}$ bacteria per g of soil (Figure 2B). Within the five wheat species, *Ae. tauschii* AT0 displayed higher levels than the three other lines of this species, whereas the other differences were not significant. Bacterial community size in the rhizosphere was higher for *T. urartu* than for *Ae. speltoides*, and for *Ae. tauschii* and *T. aestivum* than for the three other wheat

species. In bulk soil, bacterial community size was higher than in the rhizosphere of *Ae. speltoides* but lower than in the rhizosphere of *Ae. tauschii* and *T. aestivum*.

3.2. Diversity of the total bacterial community at 40 days

The *rrs* sequences obtained were grouped in 42,329 OTUs. Rarefaction curves indicated that the asymptote was reached for 99 of the 110 samples (Figure S1).

For α-diversity, the only intra-species difference was between *T. dicoccon* lines TD3 and TD9 when using the inverse Simpson index (Figure 3C). The differences between wheat species and bulk soil were not statistically significant based on Shannon or inverse Simpson indices, whereas the Chao 1 index was higher for bulk soil, *Ae. tauschii* and *T. aestivum* than for *T. urartu*, and for *T. aestivum* than for *Ae. speltoides* (Figure 3ABC).

Averaged profile of bacterial taxa abundance for each species is shown in Figure 4, as rather similar profiles were obtained for each line belonging to a same species (not shown). *Actinobacteria* and *Proteobacteria* were the most abundant phyla in the rhizosphere of all five species and in bulk soil, followed with *Acidobacteria*, *Verrucomicrobia*, *Bacteroidetes* and *Gemmatimonadetes* (Figure 4A). There were significantly more *Actinobacteria* with *T. aestivum* in comparison to *T. urartu* and *Ae. speltoides*. The relative abundance of *Bacteroidetes* was higher in the rhizosphere of *T. urartu*, *Ae. speltoides* and *T. dicoccon* compared with *Ae. tauschii* and *T. aestivum*. The 20 most abundant genera represented about half the sequences (Figure 4B), and among them the relative abundance of *Acidobacterium* was higher in bulk soil compared with the rhizosphere of the five wheat species, and that of *Conexibacter* was higher with *T. aestivum* than *T. urartu*, *Ae. speltoides* and *T. dicoccon.*

NMDS and PERMANOVA/adonis analyses showed that the bacterial communities associated with *T. urartu*, *Ae. speltoides*, *T. dicoccon*, *T. aestivum* and bulk soil were all statistically different from each other ($P < 0.05$; Table S4), whereas *Ae. tauschii* did not differ

statistically from *T. aestivum* and from bulk soil (the explanatory variable 'wheat species' accounting for 38% of the total data variation; Figure 5A; Table S4).

BCA indicated that OTUs 26 (the *Proteobacteria* genus *Pelobacter*), 83 (the *Proteobacteria* species *Azospirillum oryzae*), 550 (the *Planctomycetes* genus *Pirelulla*) and 2927 (the *Verrucomicrobia* genus *Opitutus*) were most associated with *T. dicoccon* and *T. urartu* (Figure S2A). The *Proteobacteria* OTUs 29247 (genus *Hyphomonas*), 602 (genus *Paracoccus*) and 928 (genus *Sterolibacterium*) were most associated with *Ae. tauschii* and *T. aestivum.* OTUs 872 (the *Acidobacteria* genus *Acidobacterium*) and 17229 (the *Proteobacteria* genus *Burkholderia*) were most associated with bulk soil.

3.3. Abundance of *nifH*, *acdS*, *ppdC* and *phlD*-based functional groups at 14 and 40 days

At day 14, the number of diazotrophs ranged from 5.9 to 7.9 $\log_{10}$ bacteria per g of rhizosphere soil when considering plant individuals (Figure 2C), which corresponded to a relative abundance (based on *nifH*/*rrs* ratio) of 0.0094 to 0.86 (Figure S3A). The *nifH* copy number ($\log_{10}$) was significantly higher in the rhizosphere of *T. dicoccon* than in the rhizosphere of *Ae. tauschii* and *T. aestivum* and in bulk soil (Figure 2C), whereas the *nifH*/*rrs* ratio was significantly lower in the rhizosphere of *T. aestivum* and in bulk soil than in the rhizosphere of *T. durum.* At 40 days of growth, the number of diazotrophs ranged from 4.7 to 7.4 $\log_{10}$ bacteria per g of rhizosphere soil (Figure 2D), which gave a *nifH*/*rrs* ratio from 0.0011 to 1 (Figure S3B). The number of *nifH* copies ($\log_{10}$) was not significantly different between the various wheat species, or between wheat species and bulk soil (Figure 2D), but differences between lines within *A. tauschii* and *T. aestivum* species were observed. Differences in *nifH*/*rrs* ratio between wheat species or with bulk soil were not significant either, whereas differences were found between lines, within *Ae. tauschii* and *T. dicoccon* (Figure S3B).

At day 14, the number of ACC deaminase microorganisms ranged from 5.8 to 7.4 $\log_{10}$ *acdS*$^+$ bacteria per g of rhizosphere soil (Figure 2E), which gave a relative abundance (*acdS*/*rrs* ratio) from 0.0014 to 0.32 (Figure S3C). The number of *acdS* copies ($\log_{10}$) was statistically different between *T. dicoccon*, *Ae. tauschii* and *T. aestivum*, and between individual lines within *T. dicoccon* and *T. aestivum* (Figure 2E). The *acdS*/*rrs* ratio was statistically lower in the rhizosphere of *Ae. tauschii* than in the rhizosphere of *T. aestivum* and in bulk soil, and intra-species differences between lines were observed for *T. dicoccon* and *Ae. tauschii* (Figure S3C). At 40 days of growth, the number of ACC deaminase microorganisms varied between 4.7 and 6.5 $\log_{10}$ *acdS*$^+$ microorganisms per g of rhizosphere soil (Figure 2F), which corresponded to an *acdS*/*rrs* ratio between 0.0042 and 0.059 (Figure S3D). The number of *acdS* copies ($\log_{10}$) was significantly higher in the rhizosphere of *Ae. tauschii* and *T. aestivum* compared with the rhizosphere of *T. urartu*, *Ae. speltoides*, *T. dicoccon* and in bulk soil (Figure 2F), whereas differences between wheat species were not significant in terms of relative abundance (Figure S4B).

At day 14, the number of *ppdC*$^+$ IAA producers ranged from 5.6 to 7.3 $\log_{10}$ *ppdC*$^+$ bacteria per g of rhizosphere soil (Figure 2G), corresponding to a relative abundance (based on *ppdC*/*rrs* ratio) from 0.0074 to 0.28 (Figure S3G). *ppdC* copy number ($\log_{10}$) was not significantly different between the rhizosphere of *T. dicoccon*, *Ae. tauschii* and *T. aestivum* (Figure 2G), but the *ppdC*/*rrs* ratio was significantly higher in the rhizosphere for *Ae. tauschii* compared with *T. dicoccon* and in the rhizosphere of *Ae. tauschii* and *T. aestivum* than in bulk soil (Figure S3E). At day 40, the number of *ppdC*$^+$ IAA producers was between 4.9 and 7.1 $\log_{10}$ *ppdC*$^+$ bacteria per g of rhizosphere soil (Figure 2H), giving a *ppdC*/*rrs* ratio from 0.00108 to 0.55 (Figure S3F). The number of *ppdC* copies ($\log_{10}$) was higher in the rhizosphere of *Ae. tauschii* and *T. aestivum* than in the rhizosphere of *T. urartu*, *Ae. speltoides*, *T. dicoccon* and in bulk soil (Figure 2H). The relative abundance of *ppdC*$^+$ IAA

producers was significantly higher in the rhizosphere of *Ae. tauschii* compared with the other wheats (except *T. aestivum*) and bulk soil, as well as in *T. aestivum* rhizosphere than in *T. urartu* rhizosphere. Intra-species differences were observed between lines of *Ae. tauschii* (Figure S3F).

At day 14, the number of *phlD*$^+$ bacteria was at the quantification limit (defined here as the lowest concentration at which the method is able to provide quantification, *i.e.* the lowest standard concentration giving a qPCR efficacy between 80 and 100%) of 1.20×10^3 *phlD* copies g^{-1} dry soil or below this limit for respectively 3 and 7 of 17 *T. durum* samples, 6 and 10 of 19 *Ae. tauschii* samples, 6 and 7 of 24 *T. aestivum* samples and 1 and 5 of 6 bulk soil samples, which means these bacteria could be quantified in only 7 samples of *T. dicoccon*, 3 samples of *Ae. tauschii* and 11 samples of *T. aestivum.* For each of the three species, the number of *phlD*$^+$ bacteria in these samples ranged from 10^4 to 10^6 cells g^{-1} dry soil. Quantification of *phlD*$^+$ bacteria in bulk soil was not possible (Figure S4). At day 40, *phlD*$^+$ bacteria were below detection limit for all samples.

3.4. Diversity of free nitrogen fixers at 40 days

nifH sequences obtained at 40 days were grouped in 9908 OTUs. Rarefaction curves indicated that the asymptote was reached for 97 of the 115 samples (Figure S5). α-diversity analysis of the free nitrogen fixers indicated that Chao 1 index was lower for *T. urartu* and *Ae. speltoides* than for bulk soil and *T. dicoccon*, *Ae. tauschii* and *T. aestivum*, whereas the latter three differed from one another (Figure 3D). Shannon index was lower for *T. urartu*, *Ae. speltoides*, *T. dicoccon* compared with *Ae. tauschii*, as well as *T. urartu* and *T. dicoccon* compared with *T. aestivum* (Figure 3E). Inverse Simpson index was higher for *T. urartu* and *Ae. speltoides* than *Ae. tauschii* (Figure 3F). For all three indices, intra-species differences were not significant.

Based on *nifH* data, six major classes of diazotrophs were found in the rhizosphere of the five wheat species, *i.e. Actinobacteria*, *α-Proteobacteria, β-Proteobacteria, γ-Proteobacteria, δ-Proteobacteria* and *Methanosarcina* (Figure S6A). The most abundant genera were *Geobacter, Bradyrhizobium, Pelomonas, Rhizobium* and *Streptomyces* (Figure 4C). The relative abundance profiles (based on *nifH*$^+$ genera) of *Ae. tauschii* and *T. aestivum* were similar to that of bulk soil but different from the profile of *T. urartu*, *Ae. speltoides* and *T. dicoccon*. The principal difference was a higher relative abundance of *nifH*$^+$ *Geobacter* in the rhizosphere of *Ae. tauschii* and *T. aestivum*, as well as in bulk soil compared with the rhizosphere of the three other wheats (Figure 4C). There were more *nifH*$^+$ *Streptomyces* and *Pelomonas* in the rhizosphere of *T. urartu*, *Ae. speltoides* and *T. dicoccon* than in the rhizosphere of *T. aestivum* and *Ae. tauschii*.

NMDS (Figure 5B) and PERMANOVA/adonis analyses showed that the diazotroph communities associated with *T. urartu*, *Ae. speltoides* and *T. dicoccon* did not differ ($P > 0.05$; Table S4). Bray-Curtis distances indicated that *T. urartu* and *Ae. speltoides* were the closest. *Ae. tauschii* and *T. aestivum* displayed similar diazotroph communities and differed significantly from *T. urartu*, *Ae. speltoides* and *T. dicoccon* ($P < 0.05$; Figure 5B; Table S4). *Ae. tauschii* line AT0 was very close to *T. aestivum* lines. Only *T. urartu* and *Ae. speltoides* exhibited a diazotroph community significantly different from that of bulk soil. The 'wheat species' variable explained 24% of the total variation observed.

BCA showed that the two *nifH*$^+$ OTUs 9438 (the β-*Proteobacteria* genus *Pseudoacidovorax*) and 82 (the δ-*Proteobacteria* genus *Geobacter*) were most associated with *Ae. speltoides* and *T. urartu.* The δ-*Proteobacteria* OTUs 60, 70 and 47 (corresponding also to the genus *Geobacter*) and the α-*Proteobacteria* OTUs 8 and 423 (genus *Bradyrhizobium*) were most associated with *Ae. tauschii* as well as *T. aestivum.* The OTU 71 (corresponding also to the genus *Bradyrhizobium*) was most associated with *T. dicoccon* (Figure S2B).

4. DISCUSSION

Due to several hybridization and polyploidization events, wheat genome architecture can vary drastically between wheat species, which may have an impact on root properties (Waines & Ehdaie, 2007; Pérez-Jaramillo *et al.*, 2016; Iannucci *et al.*, 2017; Roucou *et al.*, 2018; Golan *et al.*, 2018; Ahmadi *et al.*, 2018; Gruet *et al.*, 2022a). Consequently, it is expected to affect rhizosphere microbiota as well, a hypothesis that was tested in the current work. This was made possible by the availability of current representatives with AA, BB, AABB, DD and AABBDD genomic architectures, as we do not have access to the exact same wheat species or genotypes that participated in the hybridization events (Gruet *et al.*, 2022a). In addition, environmental conditions prevailing at the times of these hybridizations are not well documented, and here we chose a single set of soil and greenhouse features, based on their ability to sustain growth of the different wheat species tested, so as to focus comparisons on the genomic effects. Indeed, in the experiment the different wheats followed similar development patterns despite contrasted plant biomass (Table S3). The analysis of a large range of genotypes meant that only one soil type could be used, as done when comparing different wheat species (Ito *et al*., 2020; Kinnunen-Grubb *et al*., 2020; Spor *et al*., 2020; Tkacz *et al.*, 2020). Likewise, we used seeds produced under the same field growth conditions to avoid potential bias. Substantial variability in microbial data was observed between different lines of a same species, which could be expected since contrasted genotypes were used to consider some of the diversity existing in each species. Against this background, we sought to identify overriding effects on wheat-microorganisms interactions related to wheat genome architecture.

The first approach focused on the size of microbial functional groups important for plant growth. This was done by qPCR, as metagenomics at current sequencing depths is not as effective for genes that are not highly abundant in the community. qPCR did not prove effective for DAPG producers, which were often below the detection limit. In other rhizosphere conditions and with other counting methods, the abundance of DAPG producers was plant genotype-dependant (Mazzola *et al.*, 2004; Meyer *et al.*, 2010; Latz *et al.*, 2015). Under soilless conditions, root colonization by DAPG$^+$ *P. ogarae* F113 was higher for ancient than modern genotypes of *T. aestivum* (Valente *et al.*, 2020). *phlD* gene is only present in few species among the *Pseudomonas* (Almario *et al.*, 2017), and here only 254 of 41,165 *rrs*–based OTUs (0.62%) were affiliated to this genus. For the other functional groups, the comparison between AA (*T. urartu*), BB {SS} (*Ae. speltoides*) and AABB (*T. dicoccon*) genome representatives did not evidence any significant difference in the total amounts of *nifH*, *acdS* and *ppdC* genes at 40 days, suggesting a lack of specific impact of genome A *vs* B on the size of the corresponding functional groups (Figure 2). For the comparison between AABB (*T. dicoccon*), DD (*Ae. tauschii*) and AABBDD (*T. aestivum*) representatives, the total amount of *nifH* genes did not differ at 40 days and was lower (but by a small extent) for *T. aestivum* than for *Ae. tauschii* at 14 days. However, higher amounts of *acdS* and *ppdC* genes were found at 40 days with *Ae. tauschii* and *T. aestivum* compared with *T. dicoccon*, which suggests a particular effect of genome D. Similar effects were not observed at 14 days, even though *acdS* levels for *T. aestivum* (but not *Ae. tauschii*) exceeded those for *T. dicoccon*. This type of finding was made possible by the development of *acdS* and *ppdC* qPCR primers in recent years (Bouffaud *et al.*, 2018; Gruet *et al.*, 2022b). In parallel, higher levels with *Ae. tauschii* and *T. aestivum* compared with *T. dicoccon* (and bulk soil) were also observed for the size of the total bacterial community at 40 days (while levels in bulk and rhizosphere soils did

not differ at 14 days). This suggests that genome D effects may materialize at a wider scale in the root-associated microbiota, i.e. beyond the breadth of particular functional groups.

The second approach focused on the diversity of a key microbial functional group (N fixers), which has the potential to contribute to nitrogen nutrition of wheat (Majeed *et al.*, 2015; Dellagi *et al.*, 2020). The diversity of N fixers can vary with *Poaceae* genotype, as found in oat (Soares *et al.*, 2006), maize (Bouffaud *et al.*, 2016; Favela *et al.*, 2021) and rice (Engelhard *et al.*, 2000), but effects potentially related to plant genomic architecture are not documented. Here, the comparison between AA, BB {SS} and AABB representatives did not show any particular effect of wheat genomic profile on the diversity of this functional group, whereas *Ae. tauschii* (DD) and *T. aestivum* (AABBDD) recruited a different array of N fixers compared with *T. dicoccon* (AABB), pointing again to a particular role for genome D (Figure 5). When considering *nifH*-based OTUs in the rhizosphere, *∂-Proteobacteria* of the *Geobacteraceae* family were more prevalent with *Ae. tauschii* and *T. aestivum* than *T. dicoccon*, and especially OTUs from the genera *Geobacter* and the species *Geobacter uraniireduscens*.

When considering the wider scale of the global rhizobacterial community, differences between the AA, BB {SS} and AABB representatives (*T. urartu*, *Ae. speltoides* and *T. dicoccon*, respectively) were statistically significant, unlike in Tkacz *et al.* (2020) where the comparison focused on synthetic hybrids (rather than natural lines). Here, differences were not significant for N fixers, meaning that selection of diazotrophs was a trait conserved during the early stages of wheat evolution. Since the total bacterial community of *T. aestivum* (AABBDD) did not differ from the one of *Ae. tauschii* (DD) while being distinct from that of *T. dicoccon* (AABB), it also means that the diazotroph selection pattern of *Ae. tauschii* (shared with its descendant *T. aestivum*) paralleled selection traits that operated also at the scale of the whole community. Differences in whole bacterial community were also evidenced

524 in previous work, but with only one (Ito *et al.*, 2020) or two representatives (Wipf &
525 Coleman-Derr, 2021) for genomes BB {SS} and DD, which limited the possibility of inter-
526 species comparisons.

527 The fungal rhizosphere community is influenced by wheat genome architecture
528 (Özkurt *et al.*, 2019; Tkacz *et al.*, 2020). Thus, the presence of the D genome leads to
529 preferential selection of *Glomeromycota* fungi, as found for mycorrhizal colonization of
530 hexaploid wheat (Kapulnik & Kushnir, 1991; Hetrick *et al.*, 1992; Tkacz *et al.*, 2020). In
531 addition, several differences in stress tolerance and pathogen resistance between durum and
532 bread wheats are due to the D genome, not present in durum wheat (Saia *et al.*, 2019). For
533 example, resistance metabolites against *Fusarium* head blight involves expression of genome
534 D genes (Kage *et al.*, 2017). Here, the focus was on functional groups, and results point to
535 positive effects of the D genome on selection by hexaploid wheat of ACC deaminase
536 producers and IAA *ppdC*$^{+}$ producers, two plant-beneficial functional groups. ACC deaminase
537 producers act as an ACC sink and can lower the availability of ACC, which is the precursor of
538 ethylene in plants. High concentration of ethylene, produced in case of stress, has deleterious
539 effects on plant growth, while lower ethylene levels stimulate root elongation (Glick, 2014).
540 ACC deaminase producers can improve the growth and yield of wheat and other plants under
541 salt stress and drought conditions (Zahir *et al.*, 2009; Shakir *et al.*, 2012; Hassan *et al.*, 2014).
542 Exogenous IAA affects various plant processes, leading to cell proliferation, root system
543 branching and root elongation (Scarpella *et al.*, 2010; Overvoorde *et al.*, 2010).
544 Microorganisms producing IAA via the phenylpyruvate decarboxylase pathway have plant-
545 beneficial effects (Spaepen *et al.*, 2007a), as shown upon inoculation of wheat with the *ppdC*$^{+}$
546 PGPR *A. baldaniorum* Sp245 vs a *ppdC*$^{-}$ derivative (Spaepen *et al.*, 2007b).

547 Even if genes in hexaploid wheat are highly conserved in each of the sub-genomes A,
548 B and D, without high global dominance of transcriptional activity (Haberer *et al.*, 2016), the

genes of each genome display different expression patterns depending on plant tissue or growth stage (Soltis *et al.*, 2015; Ramirez-Gonzales *et al.*, 2018). Among transcripts recovered from 11 different wheat tissues, those of homeolog genes of the D sub-genome were more abundant than transcripts of the A and B sub-genomes, including in roots (Ramirez-Gonzales *et al.*, 2018). It is conceivable that genes or alleles of the D genome could lead to particular root properties and root exudation patterns likely to explain similarities with *Ae. tauschii* in the recruitment of specific microbial populations.

5. CONCLUSION

This work extends previous findings on the impact of wheat genome architecture on the taxonomic profile of the rhizobacterial community, by using a wider range of individual genotypes for each type of genomic architecture and complementing total bacteria community assessments with qPCR data. More importantly, we show for the first time that this impact is also significant when considering specific microbial functional groups important for plant growth, thereby validating our hypothesis. Our findings point to a significant role of the D genome originating from *Ae. tauschii*, which means that the importance of genome D would not be restricted to the case of mycorrhizal fungi (Tkacz *et al.*, 2020). Rather, it may be of prime relevance for the functioning of beneficial plant-microbe interactions at large, which opens new perspective for microbiota-targeted breeding.

ACKNOWLEDGMENTS

Funding was provided by the French Ministère de l'Enseignement Supérieur, de la Recherche et de l'Innovation, by CNRS, and by ANR project Deep Impact (ANR-20-PCPA-0004). This work made use of Serre and DTAMB platforms of FR3728 BioEnviS at Université Lyon 1.

CONFLICT OF INTEREST

The authors declare no conflict of interest.

DATA AVAILABILITY STATEMENT

Sequencing data for *rrs* and *nifH* are available on the SRA database under the BioProject numbers PRJNA798370 and PRJNA802348 respectively.

SUPPLEMENTARY MATERIAL

The Supplementary Material for this article can be found online.

REFERENCES

Achouak W, Normand P, Heulin T. 1999. Comparative phylogeny of *rrs* and *nifH* genes in the *Bacillaceae*. *International Journal of Systematic and Evolutionary Microbiology* 49: 961–967.

Ahmadi J, Pour-Aboughadareh A, Fabriki-Ourang S, Mehrabi A-A, Siddique KH. 2018. Screening wheat germplasm for seedling root architectural traits under contrasting water regimes: potential sources of variability for drought adaptation. *Archives of Agronomy and Soil Science* 64: 1351–1365.

Almario J, Bruto M, Vacheron J, Prigent-Combaret C, Moënne-Loccoz Y, Muller D. 2017. Distribution of 2,4-diacetylphloroglucinol biosynthetic genes among the *Pseudomonas* spp. reveals unexpected polyphyletism. *Frontiers in Microbiology* 8: 1218.

Asouti E, Fuller DQ. 2012. From foraging to farming in the southern Levant: the development of Epipalaeolithic and Pre-pottery Neolithic plant management strategies. *Vegetation History and Archaeobotany* 21: 149–162.

Baidouri ME, Murat F, Veyssiere M, Molinier M, Flores R, Burlot L, Alaux M, Quesneville H, Pont C, Salse J. 2017. Reconciling the evolutionary origin of bread wheat (*Triticum aestivum*). *New Phytologist* 213: 1477–1486.

Bay SK, McGeoch MA, Gillor O, Wieler N, Palmer DJ, Baker DJ, Chown SL, Greening C. 2020. Soil bacterial communities exhibit strong biogeographic patterns at fine taxonomic resolution. *mSystems* 5: e00540-20

Bernardo L, Carletti P, Badeck FW, Rizza F, Morcia C, Ghizzoni R, Rouphael Y, Colla G, Terzi V, Lucini L. 2019. Metabolomic responses triggered by arbuscular mycorrhiza enhance tolerance to water stress in wheat cultivars. *Plant Physiology and Biochemistry* 137: 203–212.

610 Bouffaud M-L, Renoud S, Dubost A, Moënne-Loccoz Y, Muller D. 2018. 1-
611 Aminocyclopropane-1-carboxylate deaminase producers associated to maize and other
612 *Poaceae* species. *Microbiome* 6: 114.
613 Bouffaud M-L, Renoud S, Moënne-Loccoz Y, Muller D. 2016. Is plant evolutionary history
614 impacting recruitment of diazotrophs and *nifH* expression in the rhizosphere? *Scientific*
615 *Reports* 6: 1-9.
616 Bray JR, Curtis JT. 1957. An ordination of the upland forest communities of southern
617 Wisconsin. *Ecological Monographs* 27: 326–349.
618 Brazelton JN, Pfeufer EE, Sweat TA, McSpadden Gardener BB, Coenen C. 2008. 2,4-
619 Diacetylphloroglucinol alters plant root development. *Molecular Plant-Microbe*
620 *Interactions* 21: 1349–1358.
621 Bru D, Ramette A, Saby NPA, Dequiedt S, Ranjard L, Jolivet C, Arrouays D, Philippot L.
622 2011. Determinants of the distribution of nitrogen-cycling microbial communities at the
623 landscape scale. *The ISME Journal* 5: 532–542.
624 Burns MJ, Nixon GJ, Foy CA, Harris N. 2005. Standardisation of data from real-time
625 quantitative PCR methods – evaluation of outliers and comparison of calibration curves.
626 *BMC Biotechnology* 5: 31.
627 Cadot S, Gfeller V, Hu L, Singh N, Sanchez-Vallet A, Glauser G, Croll D, Erb M, van der
628 Heijden M, Schlaeppi K. 2021. Soil composition and plant genotype determine
629 benzoxazinoid-mediated plant-soil feedbacks in cereals. *Plant, Cell & Environment* 44: 3732-
630 3744.
631 Callahan B, Proctor D, Relman D, Fukuyama J, Holmes S. 2015. Reproducible research
632 workflow in R for the analysis of personalized human microbiome data. In:
633 Biocomputing 2016, *Proceedings in the Pacific Symposium*, 183–194.

Caporaso JG, Lauber CL, Walters WA, Berg-Lyons D, Lozupone CA, Turnbaugh PJ, Fierer N, Knight R. 2011. Global patterns of 16S rRNA diversity at a depth of millions of sequences per sample. *Proceedings of the National Academy of Sciences of the United States of America* 108: 4516–4522.

Collavino MM, Tripp HJ, Frank IE, Vidoz ML, Calderoli PA, Donato M, Zehr JP, Aguilar OM. 2014. *nifH* pyrosequencing reveals the potential for location-specific soil chemistry to influence N_2-fixing community dynamics. *Environmental Microbiology* 16: 3211–3223.

Dellagi A, Quillere I, Hirel B. 2020. Beneficial soil-borne bacteria and fungi: a promising way to improve plant nitrogen acquisition. *Journal of Experimental Botany* 71: 4469-4479.

Edgar RC. 2013. UPARSE: highly accurate OTU sequences from microbial amplicon reads. *Nature Methods* 10: 996-998.

Edgar RC, Haas BJ, Clemente JC, Quince C, Knight R. 2011. UCHIME improves sensitivity and speed of chimera detection. *Bioinformatics* 27: 2194-2200.

Edgar RC. 2010. Search and clustering orders of magnitude faster than BLAST. *Bioinformatics* 26: 2460-2461.

Engelhard M, Hurek T, Reinhold- Hurek B. 2000. Preferential occurrence of diazotrophic endophytes, *Azoarcus* spp., in wild rice species and land races of *Oryza sativa* in comparison with modern races. *Environmental Microbiology* 2: 131–141.

Favela A, O. Bohn M, D. Kent A. 2021. Maize germplasm chronosequence shows crop breeding history impacts recruitment of the rhizosphere microbiome. *The ISME Journal* 15: 2454–2464.

Feldman M, Kislev ME. 2007. Domestication of emmer wheat and evolution of free-threshing tetraploid wheat. *Israel Journal of Plant Sciences* 55: 207–221.

659 Gaby JC, Buckley DH. 2014. A comprehensive aligned *nifH* gene database: a multipurpose
660 tool for studies of nitrogen-fixing bacteria. *Database* 2014: bau001.
661 Gaby JC, Rishishwar L, Valderrama-Aguirre LC, Green SJ, Valderrama-Aguirre A, Jordan
662 IK, Kostka JE. 2017. Diazotroph community characterization via a high-throughput *nifH*
663 amplicon sequencing and analysis pipeline. *Applied and Environmental Microbiology* 84:
664 e01512-17.
665 Gaby JC, Buckley DH. 2017. The use of degenerate primers in qPCR analysis of functional
666 genes can cause dramatic quantification bias as revealed by investigation of *nifH* primer
667 performance. *Microbial Ecology* 74: 701-708.
668 Glémin S, Scornavacca C, Dainat J, Burgarella C, Viader V, Ardisson M, Sarah G, Santoni S,
669 David J, Ranwez V. 2019. Pervasive hybridizations in the history of wheat relatives.
670 *Science Advances* 5: eaav9188.
671 Glick BR. 2005. Modulation of plant ethylene levels by the bacterial enzyme ACC
672 deaminase. *FEMS Microbiology Letters* 251: 1–7.
673 Glick BR. 2014. Bacteria with ACC deaminase can promote plant growth and help to feed the
674 world. *Microbiological Research* 169: 30–39.
675 Golan G, Hendel E, Méndez Espitia GE, Schwartz N, Peleg Z. 2018. Activation of seminal
676 root primordia during wheat domestication reveals underlying mechanisms of plant
677 resilience: Root number determines drought adaptation in wheat. *Plant, Cell &*
678 *Environment* 41: 755–766.
679 Grubbs FE. 1969. Procedures for detecting outlying observations in samples. *Technometrics*
680 11: 1–21.
681 Gruet C, Muller D, Moënne-Loccoz Y. 2022a. Significance of the diversification of wheat
682 species for the assembly and functioning of the root associated-microbiome. *Frontiers in*
683 *Microbiology* doi.org/10.3389/fmicb.2021.782135

Gruet C, Oudot A, Abrouk D, Moënne-Loccoz Y, Muller D. 2022b. Rhizosphere analysis of auxin producers harboring the phenylpyruvate decarboxylase pathway. *Applied Soil Ecology* 173: 104363.

Haas M, Schreiber M, Mascher M. 2019. Domestication and crop evolution of wheat and barley: Genes, genomics, and future directions. *Journal of Integrative Plant Biology* 61: 204–225.

Haberer G, Mayer KF, Spannagl M. 2016. The big five of the monocot genomes. *Current Opinion in Plant Biology* 30: 33–40.

Hassan W, Bano R, Bashir F, David J. 2014. Comparative effectiveness of ACC-deaminase and/or nitrogen-fixing rhizobacteria in promotion of maize (*Zea mays* L.) growth under lead pollution. *Environmental Science and Pollution Research* 21: 10983–10996.

Hetrick BAD, Wilson GWT, Cox TS. 1992. Mycorrhizal dependence of modern wheat varieties, landraces, and ancestors. *Canadian Journal of Botany* 70: 2032–2040.

Hou S, Thiergart T, Vannier N, Mesny F, Ziegler J, Pickel B, Hacquard S. 2021. A microbiota-root-shoot circuit favours *Arabidopsis* growth over defence under suboptimal light. *Nature Plants* 7: 1078-1092.

Iannucci A, Canfora L, Nigro F, De Vita P, Beleggia R. 2021. Relationships between root morphology, root exudate compounds and rhizosphere microbial community in durum wheat. *Applied Soil Ecology* 158: 103781.

Iannucci A, Fragasso M, Beleggia R, Nigro F, Papa R. 2017. Evolution of the crop rhizosphere: impact of domestication on root exudates in tetraploid wheat (*Triticum turgidum* L.). *Frontiers in Plant Science* 8: 2124.

Ito N, Mori N, Miyashita NT. 2020. Rhizospheric bacterial community structure of *Triticum* and *Aegilops* revealed by pyrosequencing analysis of the 16S rRNA gene: dominance of the A genome over the B and D genomes. *Genes & Genetic Systems* 95: 249–268.

709 Jackson SA. 2017. Epigenomics: dissecting hybridization and polyploidization. *Genome*
710 *Biology* 18: 117.
711 Kage U, Karre S, Kushalappa AC, McCartney C. 2017. Identification and characterization of
712 a fusarium head blight resistance gene *TaACT* in wheat QTL-2DL. *Plant Biotechnology*
713 *Journal* 15: 447–457.
714 Kapili BJ, Barnett SE, Buckley DH, Dekas AE. 2020. Evidence for phylogenetically and
715 catabolically diverse active diazotrophs in deep-sea sediment. *The ISME Journal* 14:
716 971–983.
717 Kapulnik Y, Kushnir U. 1991. Growth dependency of wild, primitive and modern cultivated
718 wheat lines on vesicular-arbuscular mycorrhiza fungi. *Euphytica* 56: 27–36.
719 Karimi B, Terrat S, Dequiedt S, Saby NPA, Horrigue W, Lelièvre M, Nowak V, Jolivet C,
720 Arrouays D, Wincker P, *et al.* 2018. Biogeography of soil bacteria and archaea across
721 France. *Science Advances* 4: eaat1808.
722 Ke X, Feng S, Wang J, Lu W, Zhang W, Chen M, Lin M. 2019. Effect of inoculation with
723 nitrogen-fixing bacterium *Pseudomonas stutzeri* A1501 on maize plant growth and the
724 microbiome indigenous to the rhizosphere. *Systematic and Applied Microbiology* 42:
725 248-260.
726 Klappenbach JA, Saxman PR, Cole JR, Schmidt TM. 2001. rrndb: the ribosomal RNA operon
727 copy number database. *Nucleic Acids Research* 29: 181–184.
728 Kinnunen-Grubb M, Sapkota R, Vignola M, Nunes IM, Nicolaisen M. 2020. Breeding
729 selection imposed a differential selective pressure on the wheat root-associated
730 microbiome. *FEMS Microbiology Ecology* 96: fiaa196.
731 Latz E, Eisenhauer N, Scheu S, Jousset A. 2015. Plant identity drives the expression of
732 biocontrol factors in a rhizosphere bacterium across a plant diversity gradient. *Functional*
733 *Ecology* 29: 1225–1234.

Liu W, Zhou X, Jin T, Li Y, Wu B, Yu D, Delgado-Baquerizo M. 2022. Multikingdom interactions govern the microbiome in subterranean cultural heritage sites. *Proceedings of the National Academy of Sciences of the United States of America* 119: e2121141119.

Majeed A, Abbasi MK, Hameed S, Imran A, Rahim N. 2015. Isolation and characterization of plant growth-promoting rhizobacteria from wheat rhizosphere and their effect on plant growth promotion. *Frontiers in Microbiology* 6: 198.

Marcussen T, Sandve SR, Heier L, Spannagl M, Pfeifer M, The International Wheat Genome Sequencing Consortium, Jakobsen KS, Wulff BBH, Steuernagel B, Mayer KFX, *et al.* 2014. Ancient hybridizations among the ancestral genomes of bread wheat. *Science* 345: 1250092.

Mazzola M, Funnell DL, Raaijmakers JM. 2004. Wheat cultivar-specific selection of 2,4-diacetylphloroglucinol-producing fluorescent *Pseudomonas* species from resident soil populations. *Microbial Ecology* 48: 338–348.

McMurdie PJ, Holmes S. 2013. phyloseq: An R Package for reproducible interactive analysis and graphics of microbiome census data. *PLoS ONE* 8: e61217.

Messing J. 2009. The polyploid origin of maize. In: Bennetzen JL, Hake S, eds. Handbook of maize: genetics and genomics. New York, NY: Springer, 221–238.

Meyer JB, Lutz MP, Frapolli M, Péchy-Tarr M, Rochat L, Keel C, Défago G, Maurhofer M. 2010. Interplay between wheat cultivars, biocontrol pseudomonads, and soil. *Applied and Environmental Microbiology* 76: 6196–6204.

Moënne-Loccoz Y, Mavingui P, Combes C, Normand P, Steinberg C. 2015. Microorganisms and biotic interactions. In: Environmental Microbiology: Fundamentals and Applications, 395–444.

Narula N, Kumar V, Behl RK, Deubel A, Gransee A, Merbach W. 2000. Effect of P-solubilizing *Azotobacter chroococcum* on N, P, K uptake in P-responsive wheat

759 genotypes grown under greenhouse conditions. *Journal of Plant Nutrition and Soil*
760 *Science* 163: 393–398.
761 Nemergut DR, Costello EK, Hamady M, Lozupone C, Jiang L, Schmidt SK, Fierer N,
762 Townsend AR, Cleveland CC, Stanish L, *et al.* 2011. Global patterns in the biogeography
763 of bacterial taxa. *Environmental Microbiology* 13: 135–144.
764 Nowell RW, Laue BE, Sharp PM, Green S. 2016. Comparative genomics reveals genes
765 significantly associated with woody hosts in the plant pathogen *Pseudomonas syringae*:
766 Adaptation to woody hosts in *Pseudomonas syringae*. *Molecular Plant Pathology* 17:
767 1409–1424.
768 Overvoorde P, Fukaki H, Beeckman T. 2010. Auxin control of root development. *Cold Spring*
769 *Harbor Perspectives in Biology* 2: a001537.
770 Özkan H, Willcox G, Graner A, Salamini F, Kilian B. 2011. Geographic distribution and
771 domestication of wild emmer wheat (*Triticum dicoccoides*). *Genetic Resources and Crop*
772 *Evolution* 58: 11–53.
773 Özkurt E, Hassani MA, Sesiz U, Künzel S, Dagan T, Özkan H, Stukenbrock EH. 2019.
774 Higher stochasticity of microbiota composition in seedlings of domesticated wheat
775 compared to wild wheat. *bioRxiv* 685164.
776 Parnell JJ, Berka R, Young HA, Sturino JM, Kang Y, Barnhart DM, DiLeo MV. 2016. From
777 the lab to the farm: an industrial perspective of plant beneficial microorganisms.
778 *Frontiers in Plant Science* 7: 1110.
779 Paterson AH, Bowers JE, Chapman BA. 2004. Ancient polyploidization predating divergence
780 of the cereals, and its consequences for comparative genomics. *Proceedings of the*
781 *National Academy of Sciences of the United States of America* 101: 9903–9908.
782 Pérez-de-Luque A, Tille S, Johnson I, Pascual-Pardo D, Ton J, Cameron DD. 2017. The
783 interactive effects of arbuscular mycorrhiza and plant growth-promoting rhizobacteria

784 synergistically enhance host plant defences against pathogens. *Scientific Reports* 7:
785 16409.
786 Pérez-Jaramillo J, Mendes R, Raaijmakers J. 2016. Impact of plant domestication on
787 rhizosphere microbiome assembly and functions. *Plant Molecular Biology* 90: 635–644.
788 Poly F, Ranjard L, Nazaret S, Gourbière F, Jocteur Monrozier L. 2001. Comparison of *nifH*
789 gene pools in soils and soil microenvironments with contrasting properties. *Applied and*
790 *Environmental Microbiology* 67: 2255–2262.
791 Pont C, Leroy T, Seidel M, Tondelli A, Duchemin W, Armisen D, Lang D, Bustos-Korts D,
792 Goué N, Balfourier F, *et al.* 2019. Tracing the ancestry of modern bread wheats. *Nature*
793 *Genetics* 51: 905–911.
794 Ramirez-Gonzalez RH, Borrill P, Lang D, Harrington SA, Brinton J, Venturini L, Davey M,
795 Jacobs J, ..., Uauy C. 2018. The transcriptional landscape of polyploid wheat. *Science*
796 361: eaar6089.
797 Renoud S, Bouffaud M-L, Dubost A, Prigent-Combaret C, Legendre L, Moënne-Loccoz Y,
798 Muller D. 2020. Co-occurrence of rhizobacteria with nitrogen fixation and/or 1-
799 aminocyclopropane-1-carboxylate deamination abilities in the maize rhizosphere. *FEMS*
800 *Microbiology Ecology* 96: fiaa062.
801 Roucou A, Violle C, Fort F, Roumet P, Ecarnot M, Vile D. 2018. Shifts in plant functional
802 strategies over the course of wheat domestication. *Journal of Applied Ecology* 55: 25–37.
803 Saia S, Fragasso M, De Vita P, Beleggia R. 2019. Metabolomics provides valuable insight for
804 the study of durum wheat: a review. *Journal of Agricultural and Food Chemistry* 67:
805 3069–3085.
806 Salamini F, Özkan H, Brandolini A, Schäfer-Pregl R, Martin W. 2002. Genetics and
807 geography of wild cereal domestication in the near east. *Nature Reviews Genetics* 3: 429–
808 441.

809 Scarpella E, Barkoulas M, Tsiantis M. 2010. Control of leaf and vein development by auxin.
810 *Cold Spring Harbor Perspectives in Biology* 2: a001511.
811 Shakir MA, Bano A, Arshad M. 2012. Rhizosphere bacteria containing ACC-deaminase
812 conferred drought tolerance in wheat grown under semi-arid climate. *Soil and*
813 *Environment* 31: 108–112.
814 Simmons T, Caddell D, Deng S, Colemann-Derr D. 2018. Exploring the root microbiome:
815 extracting bacterial community data from the soil, rhizosphere, and root endosphere.
816 *Journal of Visualized Experiments* 135: e57561.
817 Simonin M, Cantarel AM, Crouzet A, Gervaix J, Martins JMF, Richaume A. 2018. Negative
818 effects of copper oxide nanoparticles on carbon and nitrogen cycle microbial activities in
819 contrasting agricultural soils and in presence of plants. *Frontiers in Microbiology* 9:
820 3102.
821 Simonin M, Richaume A, Guyonnet J, Dubost A, Martins JMF, Pommier T. 2016. Titanium
822 dioxide nanoparticles strongly impact soil microbial function by affecting archaeal
823 nitrifiers. *Scientific reports* 6: 33643.
824 Simonin M, Guyonnet J, Martins JMF, Ginot Morgane, Richaume A. 2015. Influence of soil
825 properties on the toxicity of TiO_2 nanoparticles on carbon mineralization and bacterial
826 abundance. *Journal of Hazardous Materials* 283: 529-535.
827 Soares RA, Roesch LFW, Zanatta G, de Oliveira Camargo FA, Passaglia LMP. 2006.
828 Occurrence and distribution of nitrogen fixing bacterial community associated with oat
829 (*Avena sativa*) assessed by molecular and microbiological techniques. *Applied Soil*
830 *Ecology* 33: 221–234.
831 Soltis PS, Marchant DB, Van de Peer Y, Soltis DE. 2015. Polyploidy and genome evolution
832 in plants. *Current Opinion in Genetics & Development* 35: 119–125.

Soltis PS, Soltis DE. 2000. The role of genetic and genomic attributes in the success of polyploids. *Proceedings of the National Academy of Sciences of the United States of America* 97: 7051–7057.

Spaepen S, Vanderleyden J, Remans R. 2007a. Indole-3-acetic acid in microbial and microorganism-plant signaling. *FEMS Microbiology Reviews* 31: 425–448.

Spaepen S, Versées W, Gocke D, Pohl M, Steyaert J, Vanderleyden J. 2007b. Characterization of phenylpyruvate decarboxylase, involved in auxin production of *Azospirillum brasilense*. *Journal of Bacteriology* 189: 7626–7633.

Tkacz A, Pini F, Turner TR, Bestion E, Simmonds J, Howell P, Greenland A, Cheema J, Emms DM, Uauy C, *et al.* 2020. Agricultural selection of wheat has been shaped by plant-microbe interactions. *Frontiers in Microbiology* 11: 132.

Vacheron J, Desbrosses G, Bouffaud M-L, Touraine B, Moënne-Loccoz Y, Muller D, Legendre L, Wisniewski-Dyé F, Prigent-Combaret C. 2013. Plant growth-promoting rhizobacteria and root system functioning. *Frontiers in Plant Science* 4: 356.

Valente J, Gerin F, Le Gouis J, Moënne- Loccoz Y, Prigent–Combaret C. 2020. Ancient wheat varieties have a higher ability to interact with plant growth-promoting rhizobacteria. *Plant, Cell & Environment* 43: 246–260.

Větrovský T, Baldrian P. 2013. The variability of the 16S rRNA gene in bacterial genomes and its consequences for bacterial community analyses. *PLoS ONE* 8: e57923.

Waines JG, Ehdaie B. 2007. Domestication and crop physiology: roots of green-revolution wheat. *Annals of Botany* 100: 991–998.

Wei F, Coe E, Nelson W, Bharti AK, Engler F, Butler E, Kim H, Goicoechea JL, Chen M, Lee S, *et al.* 2007. Physical and genetic structure of the maize genome reflects its complex evolutionary history. *PLoS Genetics* 3: e123.

Willcox G. 2005. The distribution, natural habitats and availability of wild cereals in relation to their domestication in the Near East: multiple events, multiple centres. *Vegetation History and Archaeobotany* 14: 534–541.

Wipf HML, Coleman-Derr D. 2021. Evaluating domestication and ploidy effects on the assembly of the wheat bacterial microbiome. *PLoS ONE* 16: e0248030.

Wippel K, Tao K, Niu Y, Zgadzaj R, Kiel N, Guan R, Dahms E, Zhang P, Jensen D, Logemann E, Radutoiu S, Schulze-Lefert P, Garrido-Oter, R. 2021. Host preference and invasiveness of commensal bacteria in the Lotus and *Arabidopsis* root microbiota. *Nature Microbiology* 6: 1150-1162.

Yarza P, Yilmaz P, Pruesse E, Glöckner F, Ludwig W, Schleifer K, Whitman W, Euzéby J, Amann R, Rossello-Mora R. 2014. Uniting the classification of cultured and uncultured *Bacteria* and *Archaea* using 16S rRNA gene sequences. *Nature Reviews Microbiology* 12: 635–645.

Zahir ZA, Ghani U, Naveed M, Nadeem SM, Asghar HN. 2009. Comparative effectiveness of *Pseudomonas* and *Serratia* sp. containing ACC-deaminase for improving growth and yield of wheat (*Triticum aestivum* L.) under salt-stressed conditions. *Archives of Microbiology* 191: 415–424.

Zehr JP, McReynolds LA. 1989. Use of degenerate oligonucleotides for amplification of the *nifH* gene from the marine cyanobacterium *Trichodesmium thiebautii*. *Applied and Environmental Microbiology* 55: 2522-2526.

Zhao Y. 2014. Auxin biosynthesis. *The Arabidopsis Book* 12: e0173.

879 **Legends**

880

881 **FIGURE 1.** Simplified outline of wheat evolutionary history and place of the wheat species
882 studied. Coloured wheats (purple for wild species and blue for domesticated species) were
883 used as representatives of genomic architectures AA (*i.e. Triticum urartu*), SS (which is close
884 to BB; Pont et al. 2019) (*Aegilops speltoides*), DD (*Aegilops tauschii*), AABB (*Triticum*
885 *dicoccon*), and AABBDD (*Triticum aestivum*). A hybridization event took place 500 000
886 years ago between *T. urartu* (A genome) and the B genome donor, leading to the wild
887 tetraploid wheat *T. dicoccoides* and later to the cultivated emmer *T. dicoccon* and to *T. durum*.
888 Another hybridization took place around 10 000 years ago between *T. dicoccon* and *Ae.*
889 *tauschii* (D genome), leading subsequently to the hexaploid wheat *T. aestivum*. Wheat
890 genomes are composed of 14 (AA, BB or DD), 28 (AABB) or 42 chromosomes (AABBDD).

891

892 **FIGURE 2.** Size of the total bacterial community and of microbial functional groups in bulk
893 soil and the rhizosphere of wheat species at 14 and 40 days of growth. (A and B) Size of the
894 bacterial community at 14 (A) and 40 (B) days of growth. Raw copy numbers of *rrs* were
895 divided by 4 (i.e. corrected *rrs* numbers) to estimate bacterial numbers. Plant sequences
896 representing in the order of 0.02 $\log_{10}$ only, their impact on qPCR was negligible. (C and D)
897 Size of the diazotroph community at 14 (C) and 40 (D) days. (E and F) Size of the ACC
898 deaminase community at 14 (E) and 40 (F) days. (G and H) Size of the *ppdC*$^{+}$ IAA producer
899 community at 14 (G) and 40 (H) days. Wild wheats are portrayed in purple and domesticated
900 wheats in blue. Lines are (from left to right) TU2, TU7, TU8 for *T. urartu*, AS1, AS3, AS7,
901 AS8 for *Ae. speltoides*, TD0 (not sampled at day 14 because of insufficient development),
902 TD1, TD3, TD9 for *T. dicoccon*, AT0, AT1, AT5, AT9 for *Ae. tauschii*, and AE2, AE4, AE5,
903 AE6 for *T. aestivum*. Differences between species were assessed by a nested ANOVA and

Tukey's HSD tests, while a one-way ANOVA followed by Tukey's HSD tests was performed to compare all wheat species with bulk soil ($P < 0.05$; letters α, β and γ are used to show statistical differences). Differences between lines of a same species were studied by a nested ANOVA and Tukey's HSD tests ($P < 0.05$; letters a, b and c are used to show statistical differences).

FIGURE 3. α-Diversity of total bacterial community and free nitrogen-fixers in bulk soil and the rhizosphere of wheat species at 40 days of growth, based on *rrs* and *nifH* analysis. Chao 1 (A and D), Shannon (B and E) and inverse Simpson (InvSimpson; C and F) diversity indices were computed. Wild wheats are portrayed in purple and domesticated wheats in blue. Lines are (from left to right) TU2, TU7, TU8 for *T. urartu*, AS1, AS3, AS7, AS8 for *Ae. speltoides*, TD0, TD1, TD3, TD9 for *T. dicoccon* AT0, AT1, AT5, AT9 for *Ae. tauschii*, and AE2, AE4, AE5, AE6 for *T. aestivum*. Differences between species were assessed by a nested ANOVA and Tukey's HSD tests, while a one-way ANOVA followed by Tukey's HSD tests was performed to compare all wheat species with bulk soil ($P < 0.05$; letters α, β and γ are used to show statistical differences). Differences between lines of a same species were studied by a nested ANOVA and Tukey's HSD tests ($P < 0.05$; letters a, b and c are used to show statistical differences).

FIGURE 4. Relative abundance of bacterial taxa of the total bacterial community and free nitrogen-fixers in bulk soil and the rhizosphere of wheats, based on *rrs* and *nifH* analysis. Relative abundance of all phyla (A) and the 20 most abundant genera (B) based on *rrs* analysis. Relative abundance of genera (C) and species (D) based on *nifH* analysis.

FIGURE 5. Non-metric MultiDimensional Scaling (NMDS) of the total bacterial community and the free nitrogen-fixers in bulk soil and the rhizosphere of wheats at 40 days, based on *rrs* and *nifH* data and Bray-Curtis distances. (A) NMDS of the rhizobacterial community. (B) NMDS of the free nitrogen-fixers (B). Each point corresponds to one individual plant (replicate) of a given wheat line or one bulk soil sample, and different symbols are used for the different wheat lines. Distinct colours are used for each of the wheat species and bulk soil. Statistical ellipses (confidence interval of 95% based on assuming multivariate normal distribution) are shown for each wheat species and for bulk soil. Letters a, b, c, d and e are used to show statistical relations between wheat species and bulk soil (PERMANOVA/Adonis, $P < 0.05$).

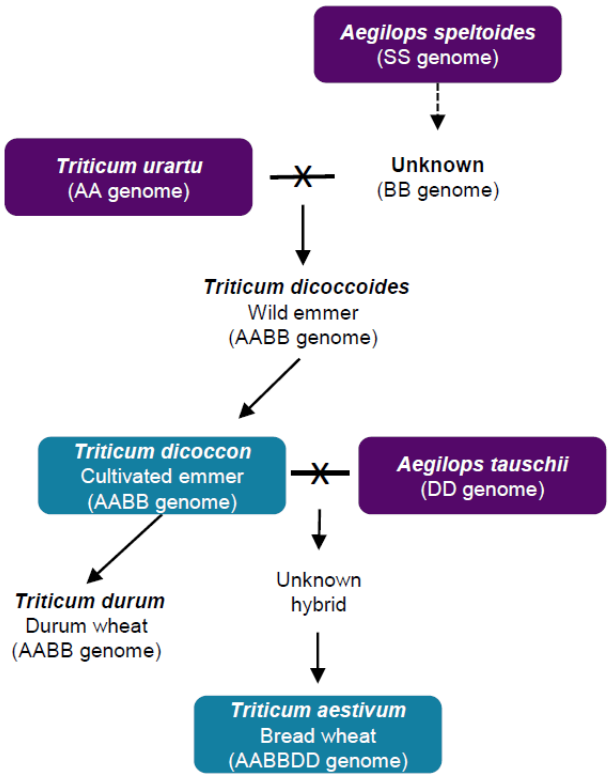

Figure 1. Simplified outline of wheat evolutionary history and place of the wheat species studied. Coloured wheats (purple for wild species and blue for domesticated species) were used as representatives of genomic architectures AA (*i.e. Triticum urartu*), SS (which is close to BB; Pont et al. 2019) (*Aegilops speltoides*), DD (*Aegilops tauschii*), AABB (*Triticum dicoccon*), and AABBDD (*Triticum aestivum*). A hybridization event took place 500 000 years ago between *T. urartu* (A genome) and the B genome donor, leading to the wild tetraploid wheat *T. dicoccoides* and later to the cultivated emmer *T. dicoccon* and to *T. durum*. Another hybridization took place around 10 000 years ago between *T. dicoccon* and *Ae. tauschii* (D genome), leading subsequently to the hexaploid wheat *T. aestivum*. Wheat genomes are composed of 14 (AA, BB or DD), 28 (AABB) or 42 chromosomes (AABBDD).

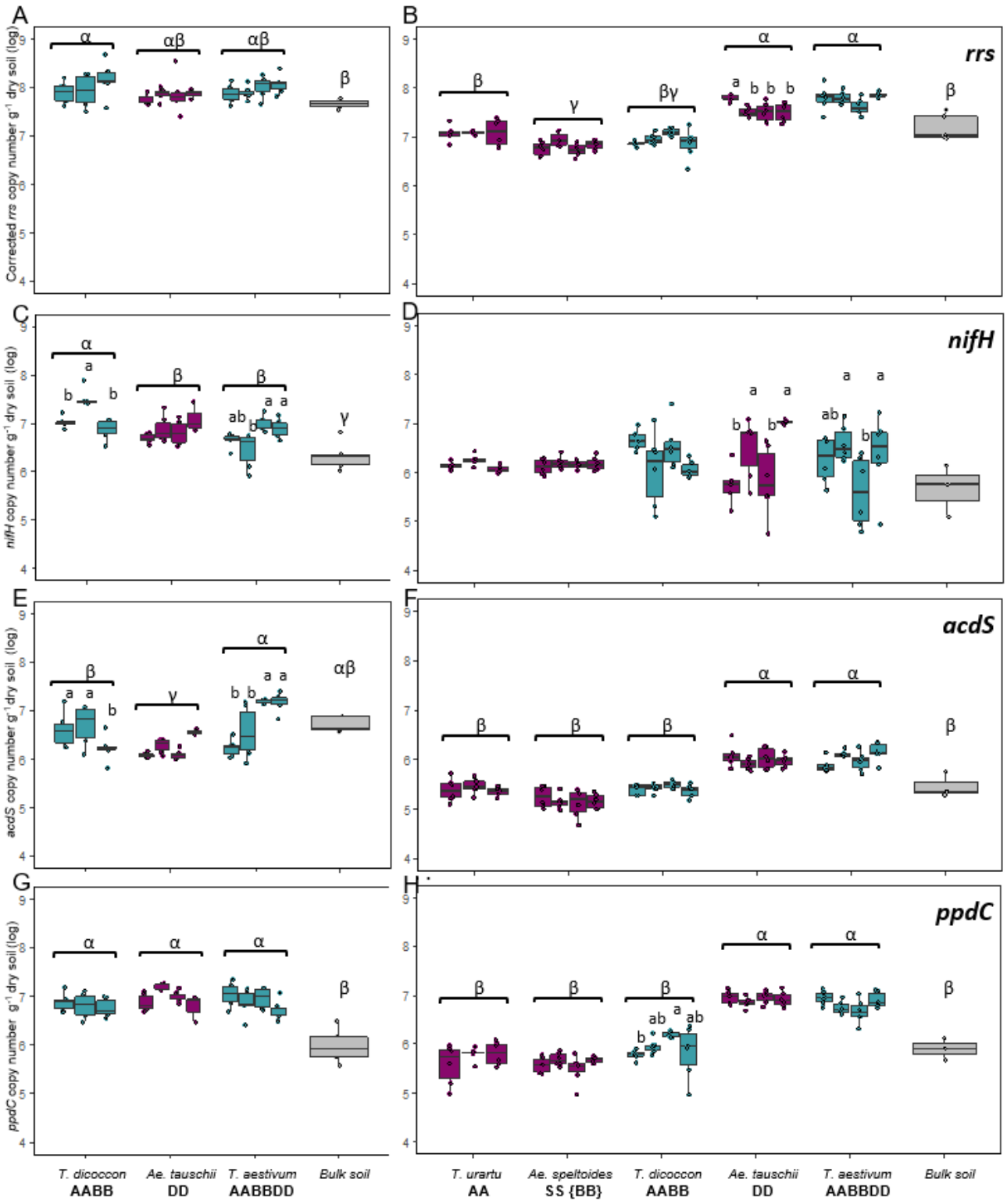

Figure 2. Size of the total bacterial community and of microbial functional groups in bulk soil and the rhizosphere of wheat species at 14 and 40 days of growth. (A and B) Size of the bacterial community at 14 (A) and 40 (B) days of growth. Raw copy numbers of *rrs* were divided by 4 (i.e. corrected *rrs* numbers) to estimate bacterial numbers. Plant sequences representing in the order of 0.02 $\log_{10}$ only, their impact on qPCR was negligible. (C and D) Size of the diazotroph community at 14 (C) and 40 (D) days. (E and F) Size of the ACC deaminase community at 14 (E) and 40 (F) days. (G and H) Size of the *ppdC*$^{+}$ IAA producer community at 14 (G) and 40 (H) days. Wild wheats are portrayed in purple and domesticated wheats in blue. Lines are (from left to right) TU2, TU7, TU8 for *T. urartu*, AS1, AS3, AS7, AS8 for *Ae. speltoides*, TD0 (not sampled at day 14 because of insufficient development), TD1, TD3, TD9 for *T. dicoccon*, AT0, AT1, AT5, AT9 for *Ae. tauschii*, and AE2, AE4, AE5, AE6 for *T. aestivum*. Differences between species were assessed by a nested ANOVA and Tukey's HSD tests, while a one-way ANOVA followed by Tukey's HSD tests was performed to compare all wheat species with bulk soil ($P < 0.05$; letters α, β and γ are used to show statistical differences). Differences between lines of a same

species were studied by a nested ANOVA and Tukey's HSD tests ($P < 0.05$; letters a, b and c are used to show statistical differences).

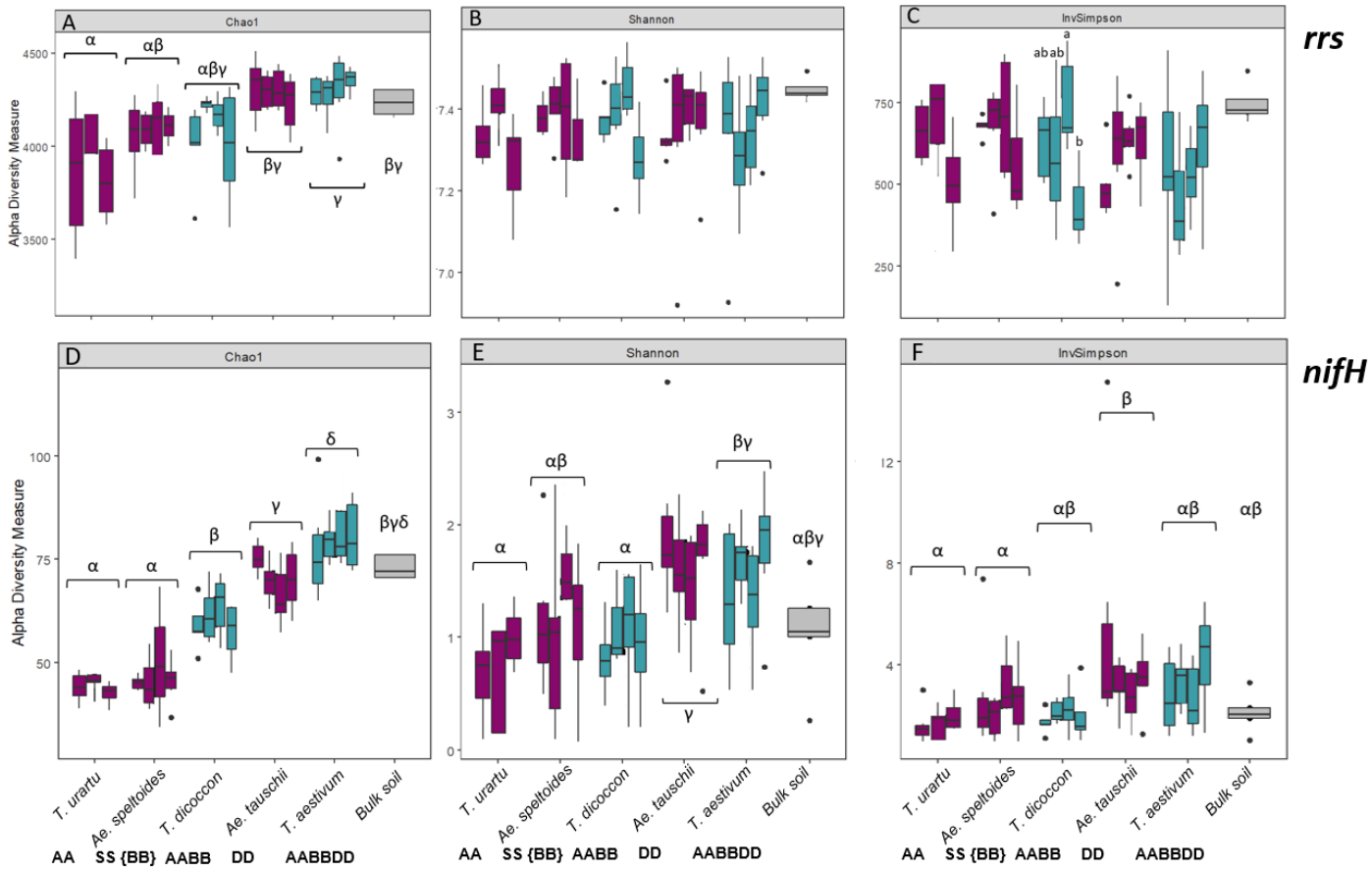

Figure 3. α-Diversity of total bacterial community and free nitrogen-fixers in bulk soil and the rhizosphere of wheat species at 40 days of growth, based on *rrs* and *nifH* analysis. Chao 1 (A and D), Shannon (B and E) and inverse Simpson (InvSimpson; C and F) diversity indices were computed. Wild wheats are portrayed in purple and domesticated wheats in blue. Lines are (from left to right) TU2, TU7, TU8 for *T. urartu*, AS1, AS3, AS7, AS8 for *Ae. speltoides*, TD0, TD1, TD3, TD9 for *T. dicoccon* AT0, AT1, AT5, AT9 for *Ae. tauschii*, and AE2, AE4, AE5, AE6 for *T. aestivum*. Differences between species were assessed by a nested ANOVA and Tukey's HSD tests, while a one-way ANOVA followed by Tukey's HSD tests was performed to compare all wheat species with bulk soil ($P < 0.05$; letters α, β and γ are used to show statistical differences). Differences between lines of a same species were studied by a nested ANOVA and Tukey's HSD tests ($P <$ 0.05; letters a, b and c are used to show statistical differences).

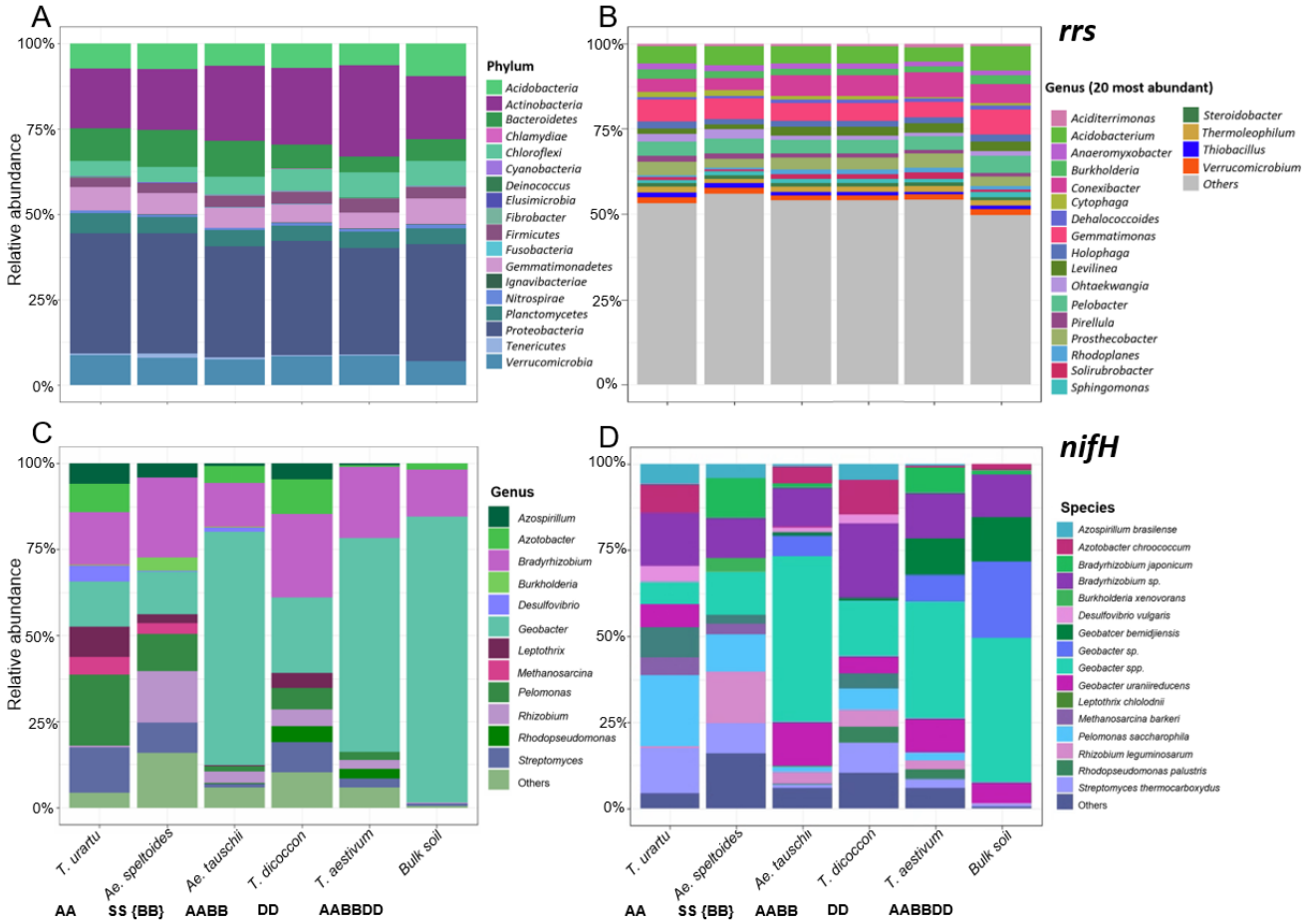

Figure 4. Relative abundance of bacterial taxa of the total bacterial community and free nitrogen-fixers in bulk soil and the rhizosphere of wheats, based on *rrs* and *nifH* analysis. Relative abundance of all phyla (A) and the 20 most abundant genera (B) based on *rrs* analysis. Relative abundance of genera (C) and species (D) based on *nifH* analysis**.**

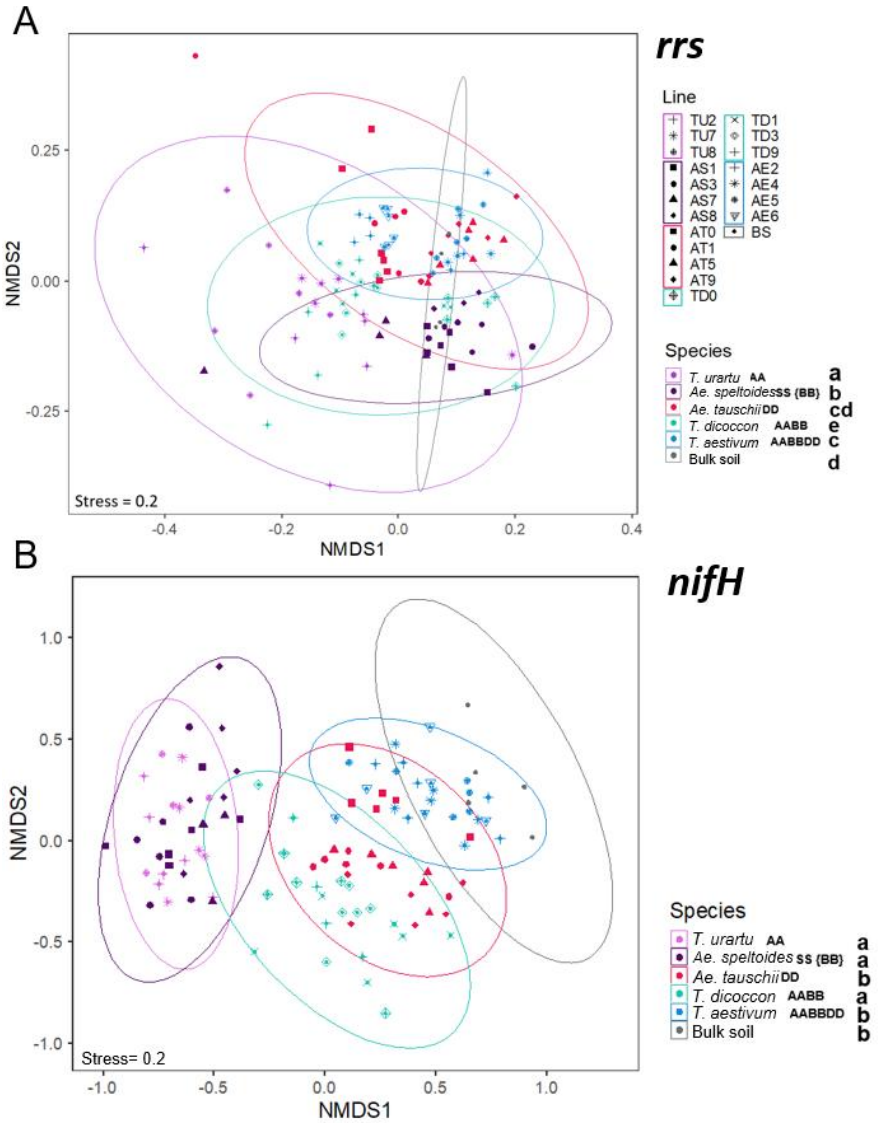

Figure 5. Non-metric MultiDimensional Scaling (NMDS) of the total bacterial community and the free nitrogen-fixers in bulk soil and the rhizosphere of wheats at 40 days, based on *rrs* and *nifH* data and Bray-Curtis distances. (A) NMDS of the rhizobacterial community. (B) NMDS of the free nitrogen-fixers (B). Each point corresponds to one individual plant (replicate) of a given wheat line or one bulk soil sample, and different symbols are used for the different wheat lines. Distinct colours are used for each of the wheat species and bulk soil. Statistical ellipses (assuming multivariate normal distribution) are shown for each wheat species and for bulk soil. Letters a, b, c, d and e are used to show statistical relations between wheat species and bulk soil (PERMANOVA/Adonis, $P < 0.05$).